

Solubility and Thermodynamics Profile of Benzethonium Chloride in Pure and Binary Solvents at Different Temperatures

Ravibhai Bhola,* Rizwan Ghumara, Chirag Patel, Vyomesh Parsana, Keyur Bhatt,* Dinesh Kundariya, and Hasit Vaghani*



Cite This: *ACS Omega* 2023, 8, 14430–14439



Read Online

ACCESS |



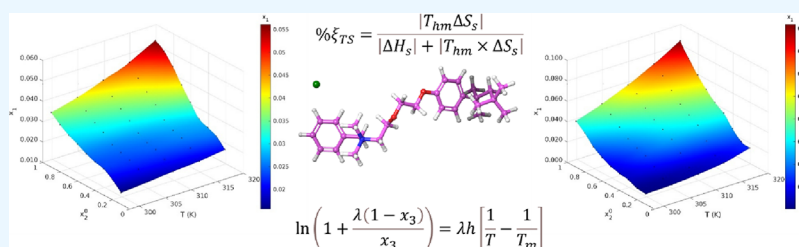
Metrics & More



Article Recommendations



Supporting Information



ABSTRACT: Benzethonium chloride (BTC) has various applications in several industries. The solubility and solution thermodynamic properties of BTC were measured. The solubility of BTC in methanol, ethanol, 1-propanol, 2-propanol, 1-butanol, water, dimethyl sulfoxide, acetic acid, and dimethyl formamide neat solvents and methanol + water and ethanol + water binary solvents at 298.15–318.15 K over an atmospheric pressure was measured. The solubility data of BTC is positively related to the temperature in all selected solvents. The solubility data was fitted by the Apelblat model, λh model, Yaws model, Van't Hoff equation, CNIBS/R-K model, and modified Jouyban–Acree equation. The RMSD and ARD were chosen to evaluate the fitting of each model. The dissolution thermodynamic parameters, enthalpy of the solution, entropy of the solution, and Gibbs energy of the solution were calculated. The solubility data and dissolution thermodynamic parameters of BTC will provide significant guidance for purification, crystallization, and separation in various areas.

1. INTRODUCTION

Benzethonium chloride (BTC; Figure 1) (IUPAC name: *N*-benzyl-*N,N*-dimethyl-2-{2-[4-(2,4,4-trimethylpentan-2-yl)-

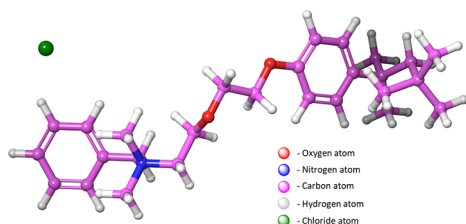


Figure 1. Molecular structure of benzethonium chloride.

phenoxy]-ethoxy}-ethylammonium chloride) contains a positively charged atom covalently bonded to four carbon atoms, one of which is a longer alkyl chain of 2-{2-[4-(2,4,4-trimethylpentan-2-yl)-phenoxy]-ethoxy} ethane, and the counter ion is a chloride anion.¹ It has antimicrobial activity against bacteria, fungi, and viruses on a broad spectrum. Several pathogens have been tested, and BTC has been shown to be highly effective against them, including methicillin-resistant *Staphylococcus aureus*, salmonella, *Escherichia coli*, *Clostridium difficile*, hepatitis B and C viruses, herpes simplex virus, HIV,

and respiratory syncytial virus. Chemical derivatives of BTC are used in a variety of products, including detergents, deodorants, astringents, creams, and antiseptics used in topical applications, cold sterilization procedures, and spermicidal applications. In addition to cosmetics, antibacterial moist towels, anti-itch ointments, mouthwashes, and antibacterial skin care products, it has also been found in a variety of other products similar to toiletries and mouthwashes. However, there is another application of BTC, namely, surface disinfection, which is found in the food industry.^{2–9}

Data of solubility and solution thermodynamics are used in various fields, such as production, purification, separation, crystallization, modification, and isolation.^{10–13} There are no reports in the literature that discuss the solubility of BTC in different solvents at varying temperatures along with the thermodynamic properties of dissolution, which motivated us to carry out the present work. The solubility of BTC in various

Received: December 12, 2022

Accepted: April 4, 2023

Published: April 14, 2023



Table 1. Experimental (x_{exp}) Mole-Fraction Solubility of BTC in Pure Solvents at a Temperature Range of 298.15–318.15 K under an Atmospheric Pressure ($p = 0.1$ MPa)^a

T (K)	χ_{exp}	10 ² RD			
		Apl.	λh	vf	Yaws
methanol					
298.15	0.0661	0.63	1.71	1.69	0.54
303.15	0.0735	-1.35	-2.03	-2.06	-1.40
308.15	0.0855	0.43	-0.78	-0.81	0.36
313.15	0.0989	0.92	0.34	0.31	0.83
318.15	0.1130	-0.48	0.64	0.61	-0.56
ethanol					
298.15	0.0393	0.11	0.05	0.00	-0.05
303.15	0.0464	-0.16	-0.42	-0.43	-0.32
308.15	0.0553	0.92	0.59	0.54	0.75
313.15	0.0639	-0.71	-0.96	-0.94	-0.88
318.15	0.0756	0.40	0.36	0.40	0.24
1-propanol					
298.15	0.0290	0.65	4.19	4.14	0.65
303.15	0.0338	-1.97	-3.93	-3.85	-1.87
308.15	0.0429	0.87	-2.75	-2.80	0.92
313.15	0.0543	0.52	-1.12	-1.10	0.52
318.15	0.0701	-0.57	3.09	3.14	-0.52
2-propanol					
298.15	0.0195	-0.01	-0.32	-13.33	0.00
303.15	0.0232	0.50	0.26	-11.21	0.43
308.15	0.0269	-0.98	-1.19	-11.52	-1.12
313.15	0.0321	0.99	0.76	-8.10	0.93
318.15	0.0369	-0.24	-0.54	-8.13	-0.27
1-butanol					
298.15	0.0236	0.50	2.31	2.12	0.37
303.15	0.0295	-0.99	-2.21	-2.03	-1.07
308.15	0.0384	0.34	-1.79	-1.82	0.24
313.15	0.0501	0.73	-0.31	-0.20	0.60
318.15	0.0651	-0.34	1.53	1.54	-0.44

T (K)	χ_{exp}	10 ² RD			
		Apl.	λh	vf	Yaws
water					
298.15	0.0085	-0.34	-5.89	-5.88	-0.52
303.15	0.0104	1.14	3.52	3.85	0.85
308.15	0.0117	0.05	4.74	5.13	-0.18
313.15	0.0125	-0.77	1.29	1.60	-0.93
318.15	0.0130	0.63	-4.97	-4.84	0.38
acetic acid					
298.15	0.0550	0.02	-1.03	-0.91	-0.16
303.15	0.0628	0.46	0.57	0.64	0.27
308.15	0.0701	-0.19	0.28	0.43	-0.37
313.15	0.0782	0.23	0.29	0.38	0.05
318.15	0.0859	0.14	-0.91	-0.81	-0.04
DMSO (dimethyl sulfoxide)					
298.15	0.0158	1.78	-0.48	-0.63	1.54
303.15	0.0183	-4.19	-3.40	-3.28	-4.45
308.15	0.0235	2.96	4.57	4.68	2.75
313.15	0.0268	0.76	1.37	1.49	0.56
318.15	0.0301	-0.62	-2.98	-2.99	-0.90
DMF (dimethyl formamide)					
298.15	0.0212	-0.55	-2.30	-6.13	-0.47
303.15	0.0265	1.31	2.15	3.40	1.13
308.15	0.0309	-1.39	0.25	5.83	-1.29
313.15	0.0368	0.26	0.99	10.33	0.27
318.15	0.0421	-0.01	-1.77	11.64	0.00

^aT is shown as the temperature in Kelvin, x_{exp} is the experimental mole fraction solubility of BTC, and Apl. (Apelblat model), λh (λh model), vf (Van't Hoff model), and Yaws (Yaws model) are values that show the relative deviation (RD). For the standard uncertainty (u), the standard uncertainty for temperature $u(T) = 0.06$ K, the relative standard uncertainty of solubility $u_{(r)}(x) = 0.04$, and the relative standard uncertainty of pressure $u_{(r)}(p) = 0.5$ KPa.

pure solvents, including methanol, ethanol, 1-propanol, 2-propanol, 1-butanol, water, dimethyl sulfoxide (DMSO), dimethyl formamide (DMF), and acetic acid, and binary solvent mixtures (methanol + water and ethanol + water) was determined using a gravimetric method at 298.15–318.15 K under an atmospheric pressure ($p = 0.1$ MPa). For the theoretical correlations, the Apelblat equation,^{14,15} the Van't Hoff equation,¹⁶ the Yaws equation,¹⁷ the λh model,¹⁸ and the modified Jouyban–Acree and CNIBS/R-K equation¹⁹ were used. Finally, the Van't Hoff model was used to determine the solution thermodynamic properties of BTC in various solvents at different temperatures.^{20,21} This dissolution thermodynamic parameter, such as the enthalpy of the solution (ΔH_s), entropy of the solution (ΔS_s), and Gibbs free energy of the solution (ΔG_s), explained dissolution behavior. The data on solubility and solution thermodynamics might be used to improve the crystallization, recrystallization, modification, and industrial production of BTC.

2. RESULTS AND DISCUSSION

2.1. Solubility Data of Benzethonium Chloride in Pure and Binary Solvents.

The experimental mole-fraction solubilities of BTC in pure solvents of methanol, ethanol, 1-propanol, 2-propanol, 1-butanol, water, DMF, DMSO, and acetic acid and in two binary solvents of methanol, ethanol, and water were measured and are listed in Tables 1 and 2. The

graphical representation of the experimental solubility is shown in Figures 2–4. In Figure 1, the solubility of all pure solvents was enhanced with respect to the temperature and in the order of the highest being methanol then acetic acid, ethanol, 1-propanol, 1-butanol, DMF, 2-propanol, DMSO, and water.

In the pure alcoholic solvents, the solubility of the solute decreases in the order of methanol, ethanol, 1-propanol, 1-butanol, and 2-propanol. The main factor in the above order might be a positive increase in the alkyl chain length of alcohol, which may be the reason for the reciprocal relationship with the solubility, except in 2-propanol. The interaction of BTC with alcoholic solvents results in a discrepancy in its solubility. We believe that, due to having one carbon in methanol, the interaction of BTC with methanol results in higher solubility, which decreases with an increase in the carbon chain. However, in the case of 2-propanol, having the hydroxyl group in the second position results in the repulsion of BTC with the solvent, resulting in a lower solubility than that of 1-butanol. Hence, the alkyl chain length and position of the hydroxyl group are the contributing factors. The polarity order is methanol (0.765) > ethanol (0.654) > 1-propanol (0.546) > 1-butanol (0.552), and the same order was found in the experimental solubility.

Figures 3 and 4 and Table 2 show the solubility of BTC in the methanol + water binary solvent system and the ethanol + water binary solvent system from 0.1 to 0.9 mole fractions

Table 2. Experimental (x_{exp}) Mole Fraction Solubility of BTC in Various Binary Solvents at Different Temperatures from 298.15 to 318.15 K under an Atmospheric Pressure ($p = 0.1 \text{ MPa}$)^a

x_2^0	$T \text{ (K)}$	x_{exp}	10^2 RD					
			Apl.	λh	vf	Yaws	CNRK	MJA
			methanol + water					
$x_2^0 = 0.1$	298.15	0.0102	-0.36	7.72	7.84	7.84	1.96	13.73
	303.15	0.0111	-0.34	-4.88	-4.50	-4.50	3.60	0.00
	308.15	0.0133	1.05	-7.53	-7.52	-7.52	3.76	-4.51
	313.15	0.0165	-1.83	-5.77	-5.45	-5.45	2.42	-4.85
	318.15	0.0232	0.39	8.57	8.42	8.42	1.51	7.99
$x_2^0 = 0.2$	298.15	0.0112	0.47	5.36	5.36	5.36	-7.14	0.89
	303.15	0.0126	-1.21	-4.15	-3.97	-3.97	-11.11	-10.32
	308.15	0.0154	0.60	-4.76	-4.55	-4.55	-11.04	-17.53
	313.15	0.0193	0.40	-2.10	-2.07	-2.07	-7.77	-10.88
	318.15	0.0251	-0.31	4.72	4.78	4.78	-4.78	-4.38
$x_2^0 = 0.3$	298.15	0.0149	-0.06	-5.10	-4.70	-4.70	6.04	3.36
	303.15	0.0197	-0.29	2.07	2.03	2.03	5.58	8.63
	308.15	0.0251	1.53	5.95	5.98	5.98	5.58	5.98
	313.15	0.0288	-1.69	0.35	0.35	0.35	2.78	4.51
	318.15	0.0332	0.65	-4.45	-4.22	-4.22	1.51	-1.20
$x_2^0 = 0.4$	298.15	0.0163	-1.10	-13.45	-13.50	-13.50	0.61	-13.50
	303.15	0.0259	2.11	8.09	8.11	8.11	6.95	10.81
	308.15	0.0341	-0.18	10.88	10.85	10.85	6.45	11.44
	313.15	0.0398	-2.14	3.27	3.27	3.27	6.78	12.06
	318.15	0.0435	1.05	-11.29	-11.26	-11.26	5.06	1.61
$x_2^0 = 0.5$	298.15	0.0188	0.01	-11.92	-11.70	-11.70	-2.13	-20.74
	303.15	0.0287	0.11	5.64	5.57	5.57	-4.18	1.39
	308.15	0.0391	1.47	11.58	11.51	11.51	-2.56	4.35
	313.15	0.0453	-1.50	3.33	3.31	3.31	-2.21	4.86
	318.15	0.0495	0.83	-11.23	-11.31	-11.31	-2.42	-6.26
$x_2^0 = 0.6$	298.15	0.0231	-0.28	-8.93	-9.09	-9.09	-1.30	-15.15
	303.15	0.0334	0.27	4.44	4.49	4.49	-5.69	0.60
	308.15	0.0441	1.25	8.91	8.84	8.84	-6.12	-0.23
	313.15	0.0511	-1.88	1.78	1.76	1.76	-5.87	0.78
	318.15	0.0577	0.80	-7.92	-7.80	-7.80	-2.95	-7.28
$x_2^0 = 0.7$	298.15	0.0289	-0.74	-7.17	-7.27	-7.27	-1.04	-4.84
	303.15	0.0403	0.56	4.22	4.22	4.22	0.50	5.96
	308.15	0.0508	-0.59	5.98	5.91	5.91	-1.38	0.20
	313.15	0.0601	-0.91	2.33	2.33	2.33	0.00	3.99
	318.15	0.0673	0.01	-6.50	-6.54	-6.54	-0.15	-4.90
$x_2^0 = 0.8$	298.15	0.0379	0.38	-3.62	-3.69	-3.69	2.90	7.12
	303.15	0.0481	-1.01	0.93	1.04	1.04	4.99	9.36
	308.15	0.0603	1.11	4.71	4.81	4.81	6.63	3.32
	313.15	0.0698	-0.31	1.33	1.29	1.29	4.73	5.87
	318.15	0.0789	0.05	-4.03	-4.06	-4.06	2.92	-1.52
$x_2^0 = 0.9$	298.15	0.0451	-0.23	0.46	0.44	0.44	-1.11	1.77
	303.15	0.0539	-0.38	-0.38	-0.37	-0.37	-2.23	0.19
	308.15	0.0645	-0.28	-0.49	-0.47	-0.47	-2.64	-10.39
	313.15	0.0771	-0.16	-0.13	-0.13	-0.13	-2.08	-2.08
	318.15	0.0918	-0.32	0.39	0.33	0.33	-1.20	-3.05
			ethanol + water					
$x_2^0 = 0.1$	298.15	0.0157	-0.20	0.17	0.00	0.00	0.00	-6.37
	303.15	0.0168	-0.03	-0.30	0.00	0.00	-0.60	-2.38
	308.15	0.0181	0.61	0.14	0.00	0.55	-0.55	0.55
	313.15	0.0191	-1.03	-1.27	-1.05	-1.05	-0.52	1.05
	318.15	0.0208	0.31	0.68	0.96	0.48	-0.96	3.37
$x_2^0 = 0.2$	298.15	0.0198	-0.33	0.64	0.51	-0.51	0.00	0.51
	303.15	0.0209	0.80	-0.01	0.00	0.96	0.96	2.39
	308.15	0.0218	-0.30	-1.66	-1.38	-0.46	0.46	1.38
	313.15	0.0232	-0.38	-1.10	-0.86	-0.43	0.86	1.29
	318.15	0.0251	0.27	1.27	1.20	0.40	2.39	1.59
$x_2^0 = 0.3$	298.15	0.0228	0.62	1.70	1.75	0.44	1.32	4.82

Table 2. continued

x_2^0	T (K)	x_{exp}	10^2 RD					
			Apl.	λh	vf	Yaws	CNRK	MJA
			ethanol + water					
$x_2^0 = 0.4$	303.15	0.0231	-0.76	-1.80	-1.73	-0.87	0.00	2.16
	308.15	0.0242	-0.11	-1.81	-1.65	-0.41	0.83	0.83
	313.15	0.0259	1.41	0.49	0.39	1.16	0.77	0.39
	318.15	0.0271	-0.47	0.66	0.74	-0.74	-0.37	-4.06
	298.15	0.0239	-0.02	1.71	1.67	-0.42	-1.67	2.09
$x_2^0 = 0.5$	303.15	0.0245	-0.15	-1.09	-1.22	0.41	-1.22	0.41
	308.15	0.0254	-0.85	-2.62	-2.36	-0.39	-1.97	-2.76
	313.15	0.0274	0.84	0.04	0.00	0.00	-1.82	-3.28
	318.15	0.0291	-0.51	1.26	1.37	-3.09	-3.78	-7.90
	298.15	0.0257	-0.52	3.89	3.89	-0.39	-0.39	1.56
$x_2^0 = 0.6$	303.15	0.0261	-0.18	-2.38	-2.30	0.00	-1.53	-1.15
	308.15	0.0277	0.17	-4.10	-3.97	0.36	-1.08	-2.53
	313.15	0.0301	-1.24	-3.12	-2.99	-1.00	-1.66	-3.32
	318.15	0.0349	0.01	4.48	4.58	0.29	1.43	0.00
	298.15	0.0281	-0.43	3.03	3.20	-0.71	1.42	1.07
$x_2^0 = 0.7$	303.15	0.0298	1.51	-0.76	-0.67	1.34	3.02	2.35
	308.15	0.0315	-0.58	-4.72	-4.76	-0.95	1.90	0.63
	313.15	0.0353	-0.32	-2.34	-2.27	-0.57	2.83	1.70
	318.15	0.0411	0.50	4.00	4.14	0.24	1.95	4.38
	298.15	0.0302	-0.60	3.52	3.64	-0.66	0.00	-2.65
$x_2^0 = 0.8$	303.15	0.0323	1.25	-1.35	-1.24	1.24	0.00	-0.62
	308.15	0.0351	0.35	-4.38	-4.27	0.28	0.85	-0.28
	313.15	0.0393	-1.65	-3.97	-3.82	-1.78	0.25	0.25
	318.15	0.0478	0.85	5.00	5.02	0.84	0.42	5.86
	298.15	0.0331	-0.81	3.28	3.32	-0.60	-0.91	-3.93
$x_2^0 = 0.9$	303.15	0.0357	1.19	-1.13	-1.12	1.40	-1.68	-1.40
	308.15	0.0388	-0.15	-4.52	-4.38	0.00	-2.06	-1.80
	313.15	0.0438	-1.57	-3.61	-3.42	-1.60	-2.05	-1.60
	318.15	0.0531	0.57	4.69	4.90	0.75	-2.07	2.45
	298.15	0.0368	0.18	1.31	1.36	-9.24	0.27	0.27
$x_2^0 = 0.9$	303.15	0.0401	0.04	-1.10	-1.00	-10.72	0.75	2.74
	308.15	0.0446	0.71	-1.10	-1.12	-11.21	0.67	3.14
	313.15	0.0493	-0.37	-1.38	-1.22	-13.59	0.81	-0.20
	318.15	0.0561	0.39	1.56	1.60	-13.90	0.89	-4.28

x_2^0 is the initial mole fraction of methanol and ethanol in the absence of a solute, T is the temperature in Kelvin, CNRK stands for the CNIBS/R-K model relative deviation, and MJA is the modified Jouyban–Acree model relative deviation. The standard uncertainty (u) is as follows: standard uncertainty for the temperature $u(T) = 0.06$ K, relative standard uncertainty of solubility $u_r(x) = 0.04$, and the relative standard uncertainty of pressure $p = 0.5$ KPa.

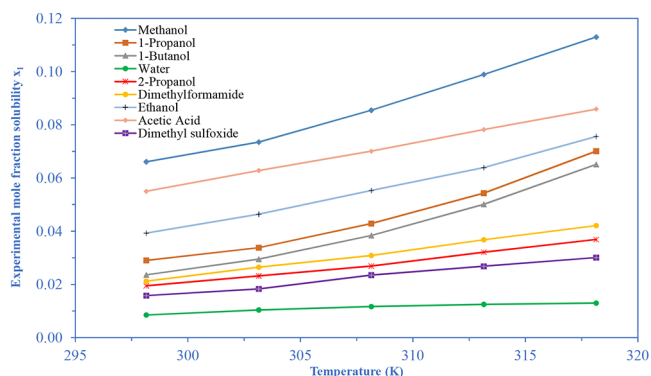


Figure 2. Experimental mole-fraction solubility (x_{exp}) of BTC in pure solvents at temperatures ranging from 298.15 to 318.15 K under an atmospheric pressure.

from $T = 298.15$ – 318.15 K at an atmospheric pressure. The experimental mole-fraction solubility of BTC in both binary

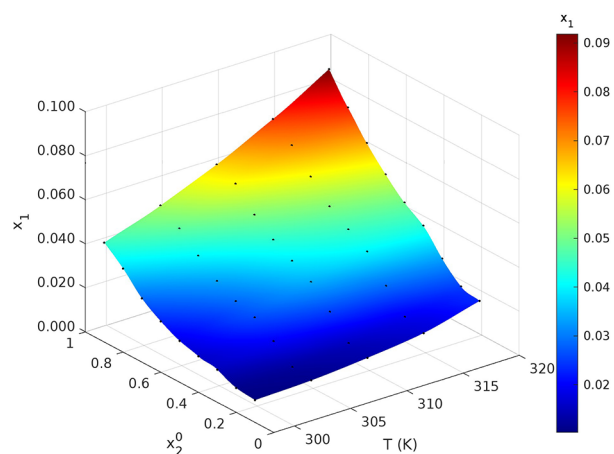


Figure 3. Experimental mole fraction solubility (x_{exp}) of BTC in methanol and water binary solvent systems at $T = 298.15$ – 318.15 K under an atmospheric pressure $p = 0.1$ MPa.

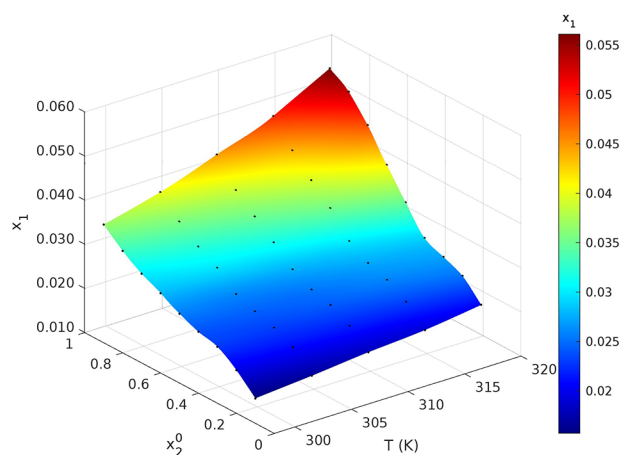


Figure 4. Experimental mole fraction solubility (x_{exp}) of BTC in the ethanol + water binary solvent at temperatures ranging from 298.15 to 318.15 K under an atmospheric pressure of $p = 0.1$ MPa.

systems demonstrates an increase with the temperature as in pure solvents. In a binary solvent system, we observe that increasing the ratio of the positive solvent results in a higher solubility. The solubility order at 318.15 K is as follows: 0.1 (0.0232), 0.2 (0.0251), 0.3 (0.0332), 0.4 (0.0435), 0.5 (0.0495), 0.6 (0.0577), 0.7 (0.0673), 0.8 (0.0789), and 0.9 (0.0918); and in the ethanol and water binary solvent system, 0.1 (0.0208), 0.2 (0.0251), 0.3 (0.0271), 0.4 (0.0291), 0.5 (0.0349), 0.6 (0.0411), 0.7 (0.0478), 0.8 (0.0531), and 0.9 (0.0561).

Solubilities in binary solvents increase with increasing the temperature and positive solvent concentration. With an increase in the amount of positive solvents or decrease in the amount of co-solvent, the interaction of solute in binary solvents lead to an increase in the interaction between the solvent and solute that may facilitate solute dissolution easier. As per dissolution molecular thermodynamics, it suggests that alcohol + water binary mixtures have two intermolecular relationships: solute–solvent cross-association and solvent–solvent cross-association. A strong solvent–solvent interaction between alcohol and BTC occurs when water is added to BTC in an alcohol solvent, resulting in a marked decrease in solubility due to a weakening of the initial intermolecular forces between BTC and alcohol. The other factors that may also affect solubility and dissolution parameters are the size and shape of the solute and solvent molecules, polarity, dipole moment, and many others.

2.2. Differential Scanning Calorimetry (DSC) Characterization. A differential scanning calorimetry analysis was carried out for the measurement of the melting temperature of BTC. A PerkinElmer Simulation Thermal Analyzer STA 8000 instrument was used, which was calibrated with standard indium and zinc under a nitrogen atmosphere at a heating rate of 10 °C/min. Approximately 3–5 mg of BTC was taken for the investigation in an aluminum pan. Figure 5 shows a DSC plot of the melting temperature of BTC where the melting peak was obtained at 437.13 K. The melting temperature of BTC is used in further thermodynamic calculations.

2.3. P-XRD Characterization. Powder XRD analysis was used to identify the nature of the solute used in the experiment. No phase transformation is observed through the powder-XRD diagram, as shown in Figure 6.

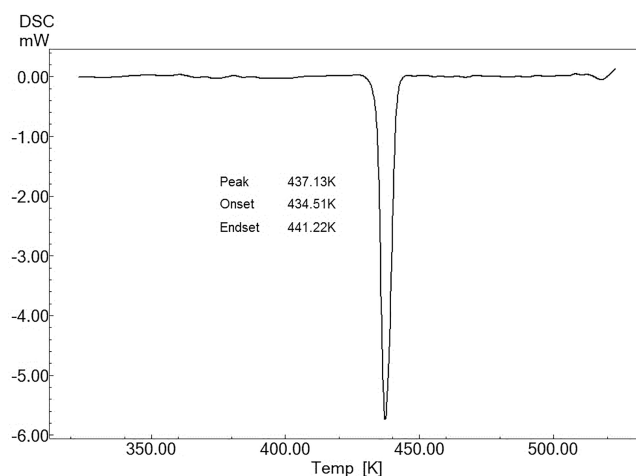


Figure 5. Differential scanning calorimetry thermogram illustrating the melting temperature of BTC.

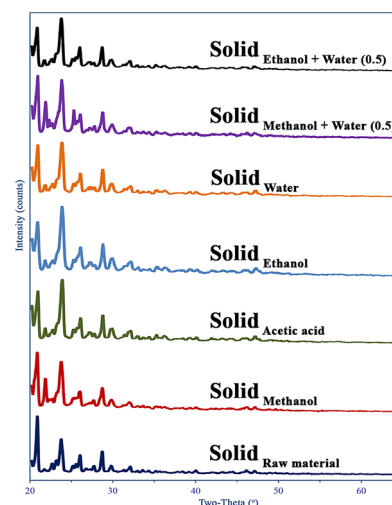


Figure 6. Powder X-ray diffraction patterns of BTC in different solvents at the room temperature and under an atmospheric pressure.

2.4. Theoretical Calculation and Correlation of Solubility. In this work, the modified Apelblat model, lh model, Yaws model, Van't Hoff model, combined nearly ideal binary solvent/Redlich-Kister model, and modified Jouyban–Acree model were used for the theoretical correlation of BTC.

2.4.1. Modified Apelblat Model. Apelblat derived an equation based on the Clausius–Clapeyron equation that predicts the theoretical solubility of various molecules.²² Equation 1 reads as follows: Apelblat model where A , B , and C are the model parameters listed in Table S1.

$$\ln x_{\text{Apl.}} = A + \frac{B}{T} + C \ln T \quad (1)$$

2.4.2. Yaws Model. The Yaws model,²⁵ eq 2, is a semi-empirical mathematical equation that can correlate the temperature and the solubility and is derived as follows where A , B , and C are the model parameters and are noted in Table S2.

$$\ln x_{\text{Yaws}} = A + \frac{B}{T} + \frac{C}{T^2} \quad (2)$$

2.4.3. CNIBS/R – K Model. The CNIBS/R – K model²⁶ is mainly used to calculate the solubility in binary liquids. This

model accurately correlates the solubility data with the solvent composition, but it does not account for the temperature. The following is a simplified version of the equation

$$\ln x_{\text{CNRK}} = B_0 + B_1x_2 + B_2x_2^2 + B_3x_2^3 + B_4x_2^4 \quad (3)$$

where B_0 – B_4 are shown as model parameters that were measured and are tabulated in Table S3.

2.4.4. Modified Jouyban–Acree Model. The Jouyban–Acree model mentioned below can be used to relate the solubility to both the solvent composition and temperature. The modified Jouyban–Acree model²⁷ is obtained from the Jouyban–Acree and modified Apelblat equations, which can be simplified as

$$\ln x = x_2 \ln(x_1)_2 + x_3 \ln(x_1)_3 + x_2 x_3 \sum_{i=0}^N \frac{J_i(x_2 - x_3)^i}{T} \quad (4)$$

$$\ln x_{\text{MJA}} = A_1 + \frac{A_2}{T} + A_3 \ln T + A_4 x_2 + A_5 \frac{x_2}{T} + A_6 \frac{(x_2)^2}{T} + A_7 \frac{(x_2)^3}{T} + A_8 \frac{(x_2)^4}{T} + A_9 x_2 \ln T \quad (5)$$

where J_i denotes the model parameters and x_1 , x_2 , and x_3 denote the mole fraction of the solute and the two pure solvents, respectively. N is the composition of the solvents, and A_1 – A_9 are the model parameters, which are recorded in Table S4.

2.4.5. λh Model. The λh model²³ proposed by Buchowski and Ksiazczak, which is widely used, has two parameters, namely, λ and h . These parameters were measured and are listed in Table 3. The mathematical representation of this model is

$$\ln \left(1 + \frac{\lambda(1 - x_1)}{x_1} \right) = \lambda h \left[\frac{1}{T} - \frac{1}{T_m} \right] \quad (6)$$

2.4.6. Van't Hoff Model. This model²⁴ is based on the principle of a solid–liquid equilibrium, and it correlates the mole fraction solubility with the temperature. The model mathematical representation is as follows where a and b are the model parameters that are listed in Table 4.

$$\ln x_{\text{vf}} = a + \frac{b}{T} \quad (7)$$

2.5. Solubility Model Correlation Result. With the help of the ARD and RMSD, all the solubility models were compared, and the data were reported. The values of the experimental mole fraction solubility and calculated mole fraction solubility of BTC in all pure and binary solvent mixtures are in good agreement. In pure solvents, the ARD% values are in the order of Apelblat (0.75) \approx Yaws (0.74) $>$ λh (1.73) $>$ Van't Hoff (3.49); in methanol and water binary solvents, the order is Yaws (0.68) \approx Apelblat (0.73) $>$ CNIBS/R – K (3.80) $>$ λh (5.30) \approx Van't Hoff (5.26) $>$ modified Jouyban–Acree (6.09), and in ethanol and water binary solvents, the order is Apelblat (0.58) $>$ CNIBS/R – K (1.14) $>$ Yaws (1.91) $>$ λh (2.11) \approx Van't Hoff (2.11) $>$ modified Jouyban–Acree model (2.21). Upon comparing the models with the percentage of the ARD data values, the Apelblat model has a higher accuracy for both pure and binary models for the theoretical calculation of mole fraction solubility of BTC. Further, all the calculated solubility data of BTC are tabulated in Tables S5 and S6.

Table 3. λh Model Parameters of BTC in Pure and Two Binary Solvents under an Atmospheric Pressure

parameters	λ	h	ARD	RMSD $\times 10^{-10}$
pure solvents				
1-propanol	2.6112	1624.130	0.0302	0.0097
1-butanol	4.1651	1164.675	0.0163	0.0022
ethanol	1.0746	2874.447	0.0048	0.0596
methanol	1.0471	2478.354	0.0110	0.0046
water	0.0738	26616.03	0.0408	0.0011
acetic acid	0.5321	3963.392	0.0061	0.0012
DMSO	0.4756	6671.594	0.0256	0.0025
DMF	0.6901	4680.548	0.0149	0.0012
2-propanol	0.5057	6003.952	0.0061	0.0209
x_2^0 (0.1 – 0.9) methanol + water				
0.1	0.5782	6648.656	0.0689	0.0067
0.2	0.6624	5827.528	0.0421	0.0027
0.3	0.8896	4238.965	0.0358	0.0052
0.4	2.4592	1856.291	0.0939	0.0005
0.5	2.7922	1634.220	0.0874	0.0006
0.6	2.5139	1709.697	0.0639	0.0004
0.7	2.2009	1808.367	0.0524	0.0004
0.8	1.6635	2102.227	0.0292	0.0002
0.9	1.6685	2022.810	0.0037	0.0321
x_2^0 (0.1 – 0.9) ethanol + water				
0.1	0.0638	20543.220	0.0051	0.8350
0.2	0.0636	17223.210	0.0094	0.0315
0.3	0.0569	15285.070	0.0129	0.0563
0.4	0.0654	14614.120	0.0134	0.0816
0.5	0.1133	12549.390	0.0359	0.0060
0.6	0.1788	9823.017	0.0297	0.0064
0.7	0.2778	7576.753	0.0364	0.0001
0.8	0.3280	6622.332	0.0344	0.0001
0.9	0.3055	6507.240	0.0129	0.0019

2.6. Dissolution Thermodynamic Analysis. The Van't Hoff equation was used to calculate the dissolution thermodynamic parameters of the dissolution enthalpy, dissolution entropy, and dissolution Gibbs free energy of BTC in pure and binary solvent mixtures of methanol + water and ethanol + water from 0.1 to 0.9 mole fractions. All the dissolution thermodynamic properties are analyzed and reported in Table 5.

According to Table 5, all these dissolution thermodynamic properties are positive in all pure solvents, all methanol and water binary solvents, and ethanol and water binary solvents (exaction in 0.2, 0.3, and 0.4 mole fractions; entropy found to be negative) observed positively, which indicates that the dissolution mechanisms are endothermic, non-spontaneous, and entropy-driven (expiation in ethanol and water of 0.2, 0.3, and 0.4).

The negative dissolution entropy observed in binary solvent systems specified in ethanol and water systems of 0.2, 0.3, and 0.4 mole fractions could be explained in the term of positive hydrophobic hydration around the non-polar groups of BTC, in particular, the alkyl groups and phenyl groups. Moreover, a similar observation is reported in the literature.^{28,29} The standard dissolution Gibbs free energy value increases with the decreasing value of the experimental mole fraction solubility of BTC. In the pure solvents, the standard Gibbs free energy of the dissolution is found to be highest in water having the lowest mole fraction solubility. The order of the Gibbs dissolution free energy in pure solvents is as follows: water

Table 4. Van't Hoff Model Parameters of BTC in Different Pure and Two Binary Solvents under an Atmospheric Pressure

parameters	<i>a</i>	<i>b</i>	ARD	RMSD × 10 ⁻¹⁰
	pure solvents			
1-propanol	10.641	-4241.13	0.0300	0.0097
1-butanol	12.500	-4851.22	0.0154	0.0021
ethanol	7.1250	-3089.62	0.0046	0.0580
methanol	5.9710	-2595.59	0.0109	0.0045
water	1.8760	-1964.20	0.0421	0.0012
acetic acid	4.1840	-2109.70	0.0063	0.0011
DMSO	6.5010	-3174.02	0.0261	0.0025
DMF	4.2090	-2386.74	0.0746	0.0004
2-propanol	5.5930	-2804.16	0.1046	0.0004
	(x_2^0) (0.1 – 0.9) methanol + water			
0.1	8.227	-3844.34	0.0675	0.0065
0.2	8.399	-3860.20	0.0414	0.0027
0.3	8.491	-3771.26	0.0345	0.0049
0.4	11.321	-4565.34	0.0940	0.0005
0.5	11.445	-4563.80	0.0868	0.0006
0.6	10.734	-4298.45	0.0640	0.0004
0.7	9.874	-3980.21	0.0525	0.0004
0.8	8.492	-3497.30	0.0298	0.0002
0.9	8.217	-3375.36	0.0034	0.0270
	(x_2^0) (0.1 – 0.9) ethanol + water			
0.1	0.237	-1310.01	0.0052	0.8235
0.2	-0.255	-1095.66	0.0095	0.0309
0.3	-0.882	-869.74	0.0131	0.0559
0.4	-0.547	-955.55	0.0135	0.0812
0.5	1.068	-1422.36	0.0357	0.0060
0.6	2.286	-1756.15	0.0296	0.0064
0.7	3.523	-2105.15	0.0362	0.0001
0.8	3.843	-2172.47	0.0341	0.0001
0.9	3.353	-1988.76	0.0127	0.0019

(11.5253), DMSO (9.7406), 2-propanol (9.2461), DMF (8.9236), 1-butanol (8.3245), 1-propanol (8.0121), ethanol (7.4411), acetic acid (6.8240), and methanol (6.2889). Moreover, the relative contributions of entropy and enthalpy are also recorded and tabulated in Table 5.

3. CONCLUSIONS

The experimental mole-fraction solubility of BTC was measured by the gravimetric method with pure solvents, specifically, methanol, ethanol, 1-propanol, 2-propanol, 1-butanol, acetic acid, DMF, DMSO, and water, and binary solvent systems of methanol and water and ethanol and water from 0.1 to 0.9 mole fractions of binary solvents at temperatures ranging from $T = 298.15$ K to $T = 318.15$ K over an atmospheric pressure. The solubility's highest rank is in the order of methanol > acetic acid > ethanol > 1-propanol > 1-butanol > DMF > 2-propanol > DMSO > water at a specified temperature and in a binary-solvent 0.9 mole fraction. The solubility of all solvents has been positively correlated with temperatures, and in the binary solvent system, it is also dependent on the positive solvents' mass fraction. Further, the Apelblat, λh , Van't Hoff, Yaws, CNIBS/R – K, and modified Jouyban–Acree models were used for the theoretical calculation. The ARD and RMSD values were found to be very small in all models with, among all models, the Apelblat model having the highest accuracy. Lastly, the dissolution thermodynamic parameters explained the endothermic and

non-spontaneous dissolution. The data obtained from this work may contribute to BTC purification, crystallization, modification, separation, and industrial production.

4. MATERIALS AND METHODS

4.1. Materials. In this present research study, chemicals such as methanol, ethanol, 1-propanol, 2-propanol, 1-butanol, DMSO, DMF, acetic acid, and water were used. The other parameters of these chemicals are listed in Table S7.

4.2. Preparations of Binary Solvent Mixtures. All the binary solvent mixtures (methanol + water and ethanol + water) were prepared by their mass using an electronic precision weight balance (Scale-Tech., SAB Classic Series) with a sensitivity of 0.001g in quantities of 30–45 g. The mole fraction in methanol and ethanol of the nine mixtures was prepared, varying from 0.1 to 0.9. The relative standard uncertainty for the preparation of binary solvents is as follows: methanol + water is $u_{(r)}(x_2^0) = 0.002$ and ethanol + water is $u_{(r)}(x_2^0) = 0.007$.

4.3. Method (Solubility Determination). Here, a gravimetric method, which has high accuracy in the determination of the solubility of many compounds, was used to measure the solubility of BTC in various pure solvents, including methanol, ethanol, 1-propanol, 2-propanol, 1-butanol, acetic acid, DMF, DMSO, and binary solvents (methanol + water and ethanol + water) within the temperature range of 298.15–318.15 K under a normal atmospheric pressure.^{30,31} The gravimetric method is simplified as follows: First, the excess amount of BTC solids was added to all selected pure and binary solvents. Then, the constant temperature of all solutions was maintained by a constant-temperature water bath with a standard error of 0.06 K. The equilibrium concentration of the solution was measured by the UV–vis spectrophotometer (Shimadzu, Model-1900). After the solution reached solid–liquid equilibrium, the upper part of the clear solution was taken by a micropipette (Lab Tech., India) with a standard uncertainty of $u = 0.01$. Then, this clear solution was added to a glass beaker that was pre-weighted using an Electronic Precision weight balance (Scale-Tech., SAB Classic Series, Model-SAB-224CL INCAL, India) with a sensitivity of 0.001g. Lastly, the glass sample beaker was put in a drying oven (Remi Electronic Tech. Ltd., Model-RDHO80, India) for the evaporation of solvents. After the complete evaporation of solvents, the final mass of residue in the glass sample beaker was noted using a Scale-Tech weight balance. All the above processes were carried out more than twice. The experimental mole-fraction solubility of BTC in pure solvents (x_{exp}) and binary solvents (x_{exp}) was calculated by mathematic eqs 1 and 2, respectively.

$$x_{\text{exp}} = \frac{\frac{m_1}{M_1}}{\frac{m_1}{M_1} + \frac{m_2}{M_2}} \quad (8)$$

$$x_{\text{exp}} = \frac{\frac{m_1}{M_1}}{\frac{m_1}{M_2} + \frac{m_2}{M_2} + \frac{m_3}{M_3}} \quad (9)$$

where x_{exp} is the mole-fraction solubility of BTC in pure and binary solvent mixtures. m_1 , m_2 , and m_3 and M_1 , M_2 , and M_3 are shown as the mass solute and solvents, respectively.

4.4. Method Validation and Literature Comparison. The solubility of sodium chloride and potassium chloride in

Table 5. Dissolution Thermodynamic Parameters of BTC in Various Pure and Binary Solvents under an Atmospheric Pressure ($p = 0.1$ MPa)^a

parameters	ΔH_s (kJ/mol)	ΔG_s (kJ/mol)	ΔS_s (J/(mol·K))	$\% \xi_H$	$\% \xi_{TS}$
pure solvents					
1-propanol	35.2597	8.0121	88.4695	56.0126	43.9874
1-butanol	40.3312	8.3245	103.922	55.3564	44.6436
ethanol	25.6819	7.4411	59.2258	58.0792	41.9208
methanol	21.5748	6.2889	49.6318	58.1392	41.8608
water	16.3287	11.5253	15.5961	76.9856	23.0144
acetic acid	17.5342	6.8240	34.7748	61.7005	38.2995
DMSO	26.3886	9.7406	54.0544	60.9340	39.0660
DMF	26.8542	8.9263	58.2099	59.5792	40.4208
2-propanol	25.2413	9.2464	51.9337	60.8285	39.1715
(x_2^0) (0.1 – 0.9) methanol + water					
0.1	31.9590	10.8954	68.3911	59.8881	40.1119
0.2	32.0920	10.5856	69.829	59.48741	40.5126
0.3	31.3521	9.6125	70.5858	58.6629	41.3371
0.4	37.9534	8.9647	94.123	56.3001	43.6999
0.5	37.9368	8.6369	95.1332	56.0265	43.9735
0.6	35.7336	8.2528	89.2267	56.1316	43.8684
0.7	33.0897	7.8073	82.0891	56.2918	43.7082
0.8	29.0741	7.3310	70.5971	56.8185	43.1815
0.9	28.0598	7.0212	68.3097	56.7554	43.2446
(x_2^0) (0.1 – 0.9) ethanol + water					
0.1	10.8913	10.2834	1.9739	94.6321	5.3679
0.2	9.1038	9.7610	-2.1339	93.2687	7.9171
0.3	7.2307	9.4896	-7.3345	76.2009	46.516
0.4	7.9440	9.3462	-4.5528	85.0008	21.858
0.5	11.8225	9.0902	8.8716	80.9805	19.0195
0.6	14.5994	8.7445	19.0102	71.0456	28.9544
0.7	17.5010	8.4782	29.2959	65.6199	34.3801
0.8	18.0580	8.2196	31.9443	64.3638	35.6362
0.9	16.5282	7.9456	27.8669	65.4578	34.5422

^aHere, ΔH_s , ΔG_s , ΔS_s , $\% \xi_H$, and $\% \xi_{TS}$ represent the dissolution enthalpy, dissolution Gibbs free energy, dissolution entropy, relative contribution enthalpy, and relative contribution entropy, respectively, of the BTC in different solvent systems. These values are obtained from eqs 11–15, respectively.

water was measured to ensure the accuracy and reliability of the measurement method used in this study. The data obtained from the sodium chloride and potassium chloride in water are represented in Table S8 and in a graphical form in Figure S2. The small difference between the experimental data value obtained from this study and previous literature indicated that the method and apparatus used in this study were reliable.

4.5. P-XRD Analysis. The power XRD analysis was carried out by the Rigaku XRD instrument model miniflex-600. The instrument had the tube voltage and current (1.54 Å⁰) set as per the standard process. The raw material of BTC and residual solid obtained from the equilibrium solution were in the test angle 2θ range of 20–80° with a scanning rate of 10°/min.

4.6. Dissolution Thermodynamic Analysis. Dissolution thermodynamic parameters such as the enthalpy of the dissolution, entropy of the dissolution, and Gibbs free energy of the dissolution were explained as were the salvation processes or mechanisms of solid solutes in various solvents, and they described an intercalation between the solute and solvent. In this present study, the various dissolution thermodynamic properties were measured by the Van't Hoff equation.^{32,33}

The harmonic temperature T_{hm} was measured by eq 10 as follows:

$$T_{hm} = \frac{n}{\sum_{i=1}^n \frac{1}{T}} \quad (10)$$

The enthalpy of the dissolution (Van't Hoff plot; Figures S3–S5), Gibb's free energy of the dissolution, and entropy of the dissolution were calculated using eqs 11, 12, and 13.

$$-\frac{H_s}{R} = \frac{d \ln x}{d \left(\frac{1}{T} - \frac{1}{T_{hm}} \right)} \quad (11)$$

$$\Delta G_s = -RT_{hm} \times \text{intercept} \quad (12)$$

$$\Delta S_s = \frac{\Delta H_s - \Delta G_s}{T_{hm}} \quad (13)$$

Lastly, the relative contribution entropy and the relative contribution enthalpy of dissolution^{34,35} are determined by eqs 14 and 15.

$$\% \xi_H = \frac{|\Delta H_s|}{|\Delta H_s| + |T_{hm} \times \Delta S_s|} \quad (14)$$

$$\% \xi_{TS} = \frac{|T_{hm} \Delta S_s|}{|\Delta H_s| + |T_{hm} \times \Delta S_s|} \quad (15)$$

4.7. Solubility Model Correlation. The average relative deviation (ARD) and the root mean square deviation (RMSD) were utilized to determine the fitting effect of the different solubility models.^{35–38} For the calculation, the following equations are used:

$$\text{ARD} = \frac{1}{n} \sum_i^n \left(\frac{x_{\text{exp}} - x_{\text{cal}}}{x_{\text{exp}}} \right) \quad (16)$$

$$\text{RMSD} = \left[\sum_{i=1}^n \left(\frac{x_{\text{cal}} - x_{\text{exp}}}{n} \right)^2 \right]^{1/2} \quad (17)$$

where x_{exp} , x_{cal} , and n signify the experimental mole-fraction solubility of BTC and the calculated mole-fraction solubility of BTC by various models and the number of observation data points, respectively.

4.8. Statistical Analysis. The experimental mole fraction solubility data and theoretical data obtained from various models in this study were carried out in Origin and MS Office software. The estimated $P < 0.05$ was taken into consideration as statistically significant.

■ ASSOCIATED CONTENT

SI Supporting Information

The Supporting Information is available free of charge at <https://pubs.acs.org/doi/10.1021/acsomega.2c07877>.

2D and 3D structures of BTC, Apelblat model parameters, Yaws model parameters, CNIBS/R – K model parameters, modified Jouyban–Acree model parameters, calculated mole fraction solubility of BTC in pure solvents, calculated mole fraction solubility of BTC in binary solvents, materials and chemical properties, literature compression and method validation, and Van't Hoff plot (PDF)

■ AUTHOR INFORMATION

Corresponding Authors

Ravibhai Bhola – Department of Chemistry, Ganpat University, Kherva 384012 Gujarat, India; orcid.org/0000-0002-1390-0441; Email: bholaravi19@gmail.com

Keyur Bhatt – Department of Chemistry, Ganpat University, Kherva 384012 Gujarat, India; Email: drkdbhatt@outlook.com, kdb01@ganpatuniversity.ac.in

Hasit Vaghani – Department of Chemistry, Ganpat University, Kherva 384012 Gujarat, India; Email: hvv01@ganpatuniversity.ac.in

Authors

Rizwan Ghumara – Department of Chemistry, Tolani College of Arts and Sciences, Adipur 370205 Gujarat, India

Chirag Patel – Department of Chemistry, Krantiguru Shyamji Krishna Verma Kachchh University, Bhuj 370001 Gujarat, India

Vyomesh Parsana – Chemical Engineering Department, VVP Engineering College, Gujarat Technological University, Rajkot 360005 Gujarat, India; orcid.org/0000-0002-7473-1354

Dinesh Kundariya – Department of Chemistry, Tolani College of Arts and Sciences, Adipur 370205 Gujarat, India

Complete contact information is available at:

<https://pubs.acs.org/10.1021/acsomega.2c07877>

Funding

The author has not received any funding grants.

Notes

The authors declare no competing financial interest.

■ ACKNOWLEDGMENTS

The authors are thankful to the MUIS Ganpat University principal for providing the basic laboratory and Maan Pharmaceuticals, Ltd. The authors are also thankful to Sagar Patel, Ajay Desai, Kinjal Joshi, and Jaymin Parikh for proof reading the manuscript for grammatical and typographical errors.

■ REFERENCES

- Malmstein, M. Surfactants and Polymers in *Drug Delivery*; Ed. Swarbrick, James, Pharmaceu Tech. Inc Pinehurst, North Carolina, USA 2002:1–26.
- Cross, J; Singer, EJ. *Cationic surfactants: analytical and biological evaluation*; vol. 53. CRC Press: 1994.
- Schreier, S.; Malheiros, S. V. P.; de Paula, E. Surface active drugs: self-association and interaction with membranes and surfactants. Physicochemical and biological aspects. *Biochim. Biophys. Acta, Biomembr.* **2000**, *1508*, 210–234.
- Yip, K. W.; Mao, X.; Au, P. Y. B.; Hedley, D. W.; Chow, S.; Dalili, S.; Mocanu, J. D.; Bastianutto, C.; Schimmer, A.; Liu, F. F. Benzethonium Chloride: A Novel Anticancer Agent Identified by Using a Cell-Based Small-Molecule Screen. *Clin. Cancer Res.* **2006**, *12*, 5557–5569.
- Paradies, H. H.; Hinze, U.; Thies, M. Hydrodynamic studies on benzethonium chloride micelles in dilute aqueous solution. *Ber. Bunsenges. Phys.* **1994**, *98*, 938–946.
- Rub, M. A.; Alabbasi, A.; Azum, N.; Asiri, A. M. Aggregation and surface phenomena of amitriptyline hydrochloride and cationic benzethonium chloride surfactant mixture in different media. *J. Mol. Liq.* **2020**, *300*, No. 112346.
- Karumbamkandathil, A.; Ghosh, S.; Anand, U.; Saha, P.; Mukherjee, M.; Mukherjee, S. Micelles of Benzethonium Chloride undergoes spherical to cylindrical shape transformation: An intrinsic fluorescence and calorimetric approach. *Chem. Phys. Lett.* **2014**, *593*, 115–121.
- Takeoka, G.; Dao, L.; Wong, R. Y.; Lundin, R.; Mahoney, N. Identification of Benzethonium Chloride in Commercial Grapefruit Seed Extracts. *J. Agric. Food Chem.* **2001**, *49*, 3316–3320.
- Coates, K. M.; Flood, P. Ketamine and its preservative, benzethonium chloride, both inhibit human recombinant $\alpha 7$ and $\alpha 4\beta 2$ neuronal nicotinic acetylcholine receptors in *Xenopus* oocytes. *Br. J. Pharmacol.* **2001**, *134*, 871–879.
- Bhola, R.; Vaghani, H.; Ghumara, R.; Bhatt, K. Drug Solubility and Dissolution Thermodynamic Approach in Various Solvents at Different Temperatures: A Review. *Biointerface Res. Appl. Chem.* **2021**, *12*, 4374–4383.
- Kolář, P.; Shen, J.-W.; Tsuboi, A.; Ishikawa, T. Solvent selection for pharmaceuticals. *Fluid Phase Equilib.* **2002**, *194–197*, 771–782.
- Bao, Y.; Xu, R.; Zhao, H. 2-Amino-6-chlorobenzoic Acid Dissolved in Numerous Individual Solvents: Equilibrium Solubility, Thermodynamic Modeling, and Mixing Properties. *J. Chem. Eng. Data* **2020**, *65*, 3252–3260.
- Bhola, R.; Ghumara, R.; Patel, C.; Parikh, J.; Desai, A.; Patel, S.; Bhatt, K.; Vaghani, H. Solubility Modeling of a Bupivacaine Hydrochloride in various solvents over a wide temperature range. *J. Chem. Eng. Data* **2023**, *68*, 744–756.
- Kalam, M. A.; Alshamsan, A.; Alkholief, M.; Alsarra, I. A.; Ali, R.; Haq, N.; Anwer, K.; Shakeel, F. Solubility Measurement and Various Solubility Parameters of Glipizide in Different Neat Solvents. *ACS Omega* **2020**, *5*, 1708–1716.
- Alshehri, S.; Hussain, A.; Ahsan, M. N.; Ali, R.; Siddique, M. U. M. Thermodynamic, Computational Solubility Parameters in Organic

Solvents and In Silico GastroPlus Based Prediction of Ketoconazole. *ACS Omega* **2021**, *6*, 5033–5045.

(16) Chen, K.; Guo, J.; Wu, Y.; Yang, Z.; Wu, B.; Ji, L. Study on Dissolution Thermodynamics and Cooling Crystallization of Rifamycin S. *ACS Omega* **2021**, *6*, 3752–3762.

(17) Qiu, J.; Wang, P.; Hu, S.; He, H.; Huang, H.; Zhao, Y.; Han, J.; Liu, H.; Guo, Y. Solubility Behavior of Boc-L-proline in 14 Pure Solvents from 283.15 to 323.15 K. *J. Chem. Eng. Data* **2021**, *66*, 2812–2821.

(18) Li, R.; Tang, T.; Yin, X.; Yao, L.; Lin, Z.; Zhang, L.; Gao, X.; Xu, X.; Zhao, J.; Han, D. Solubility of naftopidil in pure and mixed solvents at 273.15–313.15 K and its correlation with the Jouyban-Acree and CNIBS/R-K models. *J. Chem. Thermodyn.* **2020**, *145*, No. 105969.

(19) Wu, Y.; Ma, H.; Han, Y. Solubility and thermodynamic properties of piperine in (acetone/ethyl acetate + ethanol) at 278.15 K to 318.15 K and its correlation with the Jouyban-Acree and CNIBS/R-K models. *J. Chem. Thermodyn.* **2021**, *161*, No. 106555.

(20) Nair, C. P. R.; Unnikrishnan, V. Stability of the Liquid Water Phase on Mars: A Thermodynamic Analysis Considering Martian Atmospheric Conditions and Perchlorate Brine Solutions. *ACS Omega* **2020**, *5*, 9391–9397.

(21) Yu, C.; Sun, X.; Wang, Y.; Du, S.; Shu, L.; Sun, Q.; Xue, F. Determination and Correlation of Solubility of Metformin Hydrochloride in Aqueous Binary Solvents from 283.15 to 323.15 K. *ACS Omega* **2022**, *7*, 8591–8600.

(22) Shakeel, F.; Haq, N.; Alanazi, F. K.; Alanazi, S. A.; Alsarra, I. A. Solubility of sinapic acid in various (Carbitol + water) systems: computational modeling and solution thermodynamics. *J. Therm. Anal. Calorim.* **2020**, *142*, 1437–1446.

(23) Wang, Z.; Yu, S.; Li, H.; Liu, B.; Xia, Y.; Guo, J.; Xue, F. Solid–Liquid Equilibrium Behavior and Solvent Effect of Gliclazide in Mono- and Binary Solvents. *ACS Omega* **2022**, 37663.

(24) Shakeel, F.; Haq, N.; Alsarra, I. A.; Alshehri, S. Solubility, Hansen Solubility Parameters and Thermodynamic Behavior of Emtricitabine in Various (Polyethylene Glycol-400 + Water) Mixtures: *Computational Modeling and Thermodynamics. Molecules* **2020**, *25*, 1559.

(25) Alyamani, M.; Alshehri, S.; Alam, P.; Ud Din Wani, S.; Ghoneim, M. M.; Shakeel, F. Solubility and solution thermodynamics of raloxifene hydrochloride in various (DMSO + water) compositions. *Alexandria Eng. J.* **2022**, *61*, 9119–9128.

(26) Ma, J.; Huang, X.; Wang, N.; Li, X.; Bao, Y.; Wang, T.; et al. Solubility and thermodynamic mixing and dissolution properties of empagliflozin in pure and binary solvent systems. *J. Mol. Liq.* **2020**, *309*, No. 113004.

(27) Vahdati, S.; Shayanfar, A.; Hanaee, J.; Martínez, F.; Acree, W. E., Jr.; Jouyban, A. Solubility of Carvedilol in Ethanol + Propylene Glycol Mixtures at Various Temperatures. *Ind. Eng. Chem. Res.* **2013**, *52*, 16630–16636.

(28) Tinjaca, D. A.; Martínez, F.; Almanza, O. A.; Jouyban, A.; Acree, W. E., Jr. Solubility of Meloxicam in aqueous binary mixture of formamide, N-methylformamide, and N,N-dimethylformamide: Determination correlation, thermodynamics and preferential solvation. *J. Chem. Thermodyn.* **2020**, *154*, No. 106332.

(29) Tinjaca, D. A.; Martínez, F.; Almanza, O. A.; Jouyban, A.; Acree, W. E., Jr. Solubility of Meloxicam in (Carbitol + water) mixture; Determination, correlation, dissolution thermodynamics. *J. Mol. Liq.* **2020**, DOI: 10.106/j.molliq.2020.114671.

(30) Delgado, D. R.; Bahamón-Hernandez, O.; Cerquera, N. E.; Ortiz, C. P.; Martínez, F.; Rahimpour, E.; et al. Solubility of sulfadiazine in (acetonitrile + methanol) mixtures: Determination, correlation, dissolution thermodynamics and preferential solvation. *J. Mol. Liq.* **2021**, *322*, No. 114979.

(31) Barzegar-Jalali, M.; Jouyban, A.; Shekaari, H.; Martínez, F.; Mirheydari, S. N. The effect of 1-hexyl-3-methylimidazolium bromide ionic liquid as a co-solvent on the aqueous solubility of lamotrigine at T = (293.2–313.2) K. *J. Chem. Thermodyn.* **2019**, *133*, 261–271.

(32) Jouyban, A.; Nozohouri, S.; Martínez, F. Solubility of celecoxib in {2-propanol (1) + water (2)} mixtures at various temperatures: Experimental data and thermodynamic analysis. *J. Mol. Liq.* **2018**, *254*, 1–7.

(33) Tian, N.; Yu, C.; Du, S.; Lin, B.; Gao, Y.; Gao, Z. Solubility Measurement and Data Correlation of Isatoic Anhydride in 12 Pure Solvents at Temperatures from 288.15 to 328.15 K. *J. Chem. Eng. Data* **2020**, *65*, 2044–2052.

(34) Wei, J.; Chen, S.; Fu, H.; Wang, X.; Li, H.; Lin, J.; Xu, F.; He, C.; Liang, X.; Tang, H.; Shu, G. Measurement and correlation of solubility data for atorvastatin calcium in pure and binary solvent systems from 293.15 K to 328.15 K. *J. Mol. Liq.* **2021**, *324*, No. 115124.

(35) Shakeel, F.; Bhat, M. A.; Haq, N.; Fathi-Azarbayjani, A.; Jouyban, A. Solubility and thermodynamic parameters of a novel anticancer drug (DHP-5) in polyethylene glycol 400 + water mixtures. *J. Mol. Liq.* **2017**, *229*, 241–245.

(36) Bhola, R.; Vaghani, H.; Bhatt, K.; Parikh, J.; Ghumara, R. An Investigation into the Solubility and Solution Thermodynamics of Cefpodoxime Proxetil in Different Solvents that Vary with Temperature. *Chem. Afr.* **2022**, *5*, 899–905.

(37) Bhola, R.; Modi, H.; Patel, C.; Vaghani, H.; Bhatt, K.; Ghumara, R. Solubility and solution thermodynamics of 2, 6-bis (4-hydroxybenzylidene) cyclohexanone in pure and binary solvents at various temperatures. *J. Indian Chem. Soc.* **2022**, *99*, No. 100427.

(38) Liu, F.; Qu, H.; Wan, X.; Han, D.; Li, W.; Wu, S. Solubility and Data Correlation of β -Arbutin in Different Monosolvents from 283.15 to 323.15 K. *J. Chem. Eng. Data* **2019**, *64*, 5688–5697.